Seismic Response Of Tunnels In Rockmass Without Joint and in Jointed rockmass

Ambika Srivastav[1]and Neelima Satyam[2]

[1] Research Scholar, IIIT Hyderabad, EERC, ambika.srivastav@gmail.com
[2] *Associate Professor, Discipline of Civil Engineering, IIT Indore,*
neelima.satyam@iiti.ac.in

Abstract. Himalayan geology is highly influenced by rock formations of different ages and represents a mixed lithology. Changes in geological conditions are therefore frequent in Himalayan tunnels and flexible rock support methods are required to deal with constant variation of rock mass properties. The level of precision in foreseeing, assessing, and translating the nature of rockmass along the tunnel alignment is in this way a key for the effective fulfillment of any hydropower venture. This paper assesses and compares the effects of seismicity in the tunnels for the predicted and actual rock mass conditions of the recently constructed hydro-tunnels.In this study, numerical modelling approach has been used to analyze circular tunnels using the Phase2 software. The models were simulated in as the earlier models by Bhasin and others in 2006. The effect of discontinuities was investigated .The seismic loads were applied in the form of quasi-static loads and generated in different directions and combinations for each model**.**

Keywords: Jointed rockmass, Tunneling, Rock support, Seismic Loading.

1 Introduction

Recent severe damage to mountain tunnels has shown that this is not always the case. For example, following the 1999 Chi-Chi Earthquake in Taiwan (Wang et al. 2001) and the 2008 Wenchuan Earthquake in Sichuan (Li 2008), in quite a few mountain tunnels cracks appeared, linings collapsed, and there was even bending of steel. That provided new stimulus for seismic design of mountain tunnels. The main failure mechanism leading to the damages are: (1) ground failures such as landslides at portals, liquefaction and displacement of tunnels due to fault-slip, when the tunnel intercepts an active fault and (2) damage due to ground shaking resulting in lining cracks and spalling. The investigation of seismic reaction might be drawn closer by numerous strategies, for example, static methodology, pseudo-static methodology, and dynamic methodology. The pseudo-static methodology has increased more prevalence because of its simplistic approach. The main aim of this paper is to study the impact of earthquake loading, due to ground shaking, which affects the whole tunnel length from ovaling of the tunnel cross section. Three sedimentary rock mass classes with different Q value which represent "very poor" to "very good" rock masses are modeled by varying the deformation modulus and Mohr-Coulomb parameters, determined from empirical relations. The increase in support pressure (represented by axial force) is investigated as function of rock mass quality Q and tunnel dimension. A series of pseudo-static finite element analyses were performed to evaluate the the seismic response of circular tunnels in jointed rockmass. Effect of jointed rock on tunneling has been a topic of interest(Barton, 1995). Researchers used the discrete element method to investigate how the joints influence the tunnel (Bhasin and Høeg,1998; Hao and Azzam, 2005; Vardakos et al., 2007). Studies on the influence of jointed rock mass on blast induced vibration propagation have been performed. Hao et al. (2001) used the measured motions under in-situ blasting to identify the effect of the joint layout on propagation of stress waves. Li and Ma (2010) studied the interaction between the blast wave and arbitrarily positioned rock joint. Ma and Brady (1999) investigated the performance of an underground excavation in jointed rock under repeated loading.

1.1 Numerical Modelling

The plane-strain two-dimensional model of a circular tunnel of dia. 6m and 12m respectively excavated within a rock mass with Q ranges 1, 10 and 30 are considered. The main assumption in a plane-strain model is that the tunnel under consideration is infinitely long and dis-

placement is restricted to the 2D plane, which is perpendicular to the tunnel axis. While using numerical modelling to study the failure of rock masses, especially for elasto-plastic models, after choosing the failure criterion, it is imperative to specify the post-failure characteristics. Depending on the rock mass quality and stress conditions, the common post failure behaviours for elastic-plastic models are elastic-perfectly-plastic, strain-softening, and elastic-brittle-plastic. Although no fixed rule exists for the choice of the post-failure characteristics, Hoek and Brown (1997) suggested these as starting points: elastic-brittle-plastic for very good quality hard rock mass (GSI > 75) strain-softening for average quality rock mass (GSI~25 to 75) and elastic-perfectly-plastic for very poor quality rock mass (< 25 GSI). The rockmass used for this study were assumed to behave as elastic-perfectly-plastic materials.

1.1 Model Geometry and Mesh Details

The construction of a geomechanical model in Phase2 starts with specifying the shape and dimension of the tunnel. In all the experiments, the model of a circular tunnel with specified diameter is considered. For all the experiments to investigate the influence of rock mass quality, tunnel dimension, and magnitude and direction of seismic coefficient, the depth of the tunnel is fixed at 100m. This depth was chosen as most of the tunnel lie at an average depth of around 100 m (Dowding, 1979; Bhasin, 2011).

A parametric study was conducted to study the effect of seismicity on tunnels with single joints in different orientations. A series of pseudo-static finite element analyses were performed to evaluate the effect of deformation along rock joint on the seismic response of circular tunnels. The joint stiffness and shear strength have crucial influence on the tunnel response. The tunnel reaction is highest for vertical and horizontal joints and the lowest when the joint dips at an angle of 45°. Figure 1 illustrates the computational domain and the boundary conditions applied in this study. The lower boundary was fixed in the vertical and horizontal directions, whereas the lateral boundaries were fixed in the vertical direction. The tunnel was modelled as a circular opening at the centre of the field with a radius of 6 m and 12m respectively. A 0.1 m thick liner was inscribed around the circumference of the tunnel. Plane strain condition was used in all analyses. The vertical in-situ stress was considered to be litho static (based on the weight of the rock above) and for sake of simplicity, hydrostatic condition is assumed. The depth of the excavation has been kept at 100 m from the surface, a horizontal seismic coefficient of 0.3 and a downward vertical seismic coefficient of -0.2 (negative for downward direction) have been adopted. The axial force developed in the lining under static loading and seismic loading conditions have been checked for three different values of rock mass quality Q. Three sedimentary rock mass classes with different Q value which represent "very poor"(Q = 1) to "very good" rock masses (Q = 30). The effect of discontinuities was studied under the static and seismic conditions of loading and the same types of materials. Mohr-Coulomb failure criterion was employed to describe the behavior of the rocks under loading. The unit weight for the rock was set to 0.026 (MN/m³). The discontinuities were described as joints in Phase 2 program. The joints were described by Mohr-Coulomb slip criterion. Neither groundwater pore pressure nor any additional pressures were added into the joints. The geotechnical parameters assigned for rock mass and joints are shown in Table 1 and Table 2 respectively. The models were all run for elastic-perfectly plastic mediums and for both; the static and the dynamic (seismic) cases of loading.
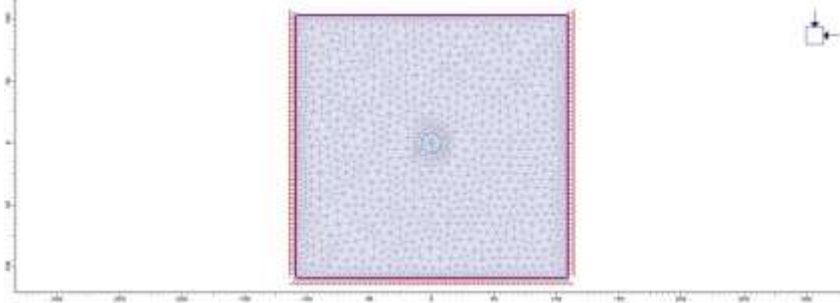
Figure 1 Phase2 Model

Geotechnical data

The vertical in-situ stress was considered to be litho static (based on the weight of the rock above) and for sake of simplicity, hydrostatic condition is assumed. A horizontal seismic coefficient of 0.3 and a downward vertical seismic coefficient of -0.2 (negative for downward direction) have been adopted. The geotechnical parameters assigned for this study are shown in Table 1 and 2 below.

Table 1 Geotechnical Parameters for rockmass

Q value	$E_{rockmass}$(GPa)	Cohesion (MPa)	Friction (Degree)
30	10.78	1.7	51
10	8.3	1.1	50.5
1	3.5	0.6	44.8

Table 2 Geotechnical Parameters for Joints

Parameter	Value
Cohesion	0
Friction	20° and 10°
Normal Stiffness	10,0000 MPa/m
Shear Stiffness	10,000 MPa/m

Influence of Tunnel Dimension

In order to examine the influence of size of tunnels on the force generated in the lining due to earthquake loading, different tunnel sizes varying from 6m dia. to 12m dia. have been considered. The depth of the excavation has been kept at 100 m from the surface and the rock mass parameters have been adopted same as the previous case for the elastic-perfectly plastic rock types.

Sequence of excavation and support installation

In the present analysis, the process of excavation and support installation was simulated with reasonable detail. Stage 1 represents the boundary of the unexcavated Tunnel modelled under hydrostatic condition, stage 2 represents the stress relaxation stage, stage 3 represents the tunnel after installation of shotcrete liner, and stage 4 represents seismic loading.
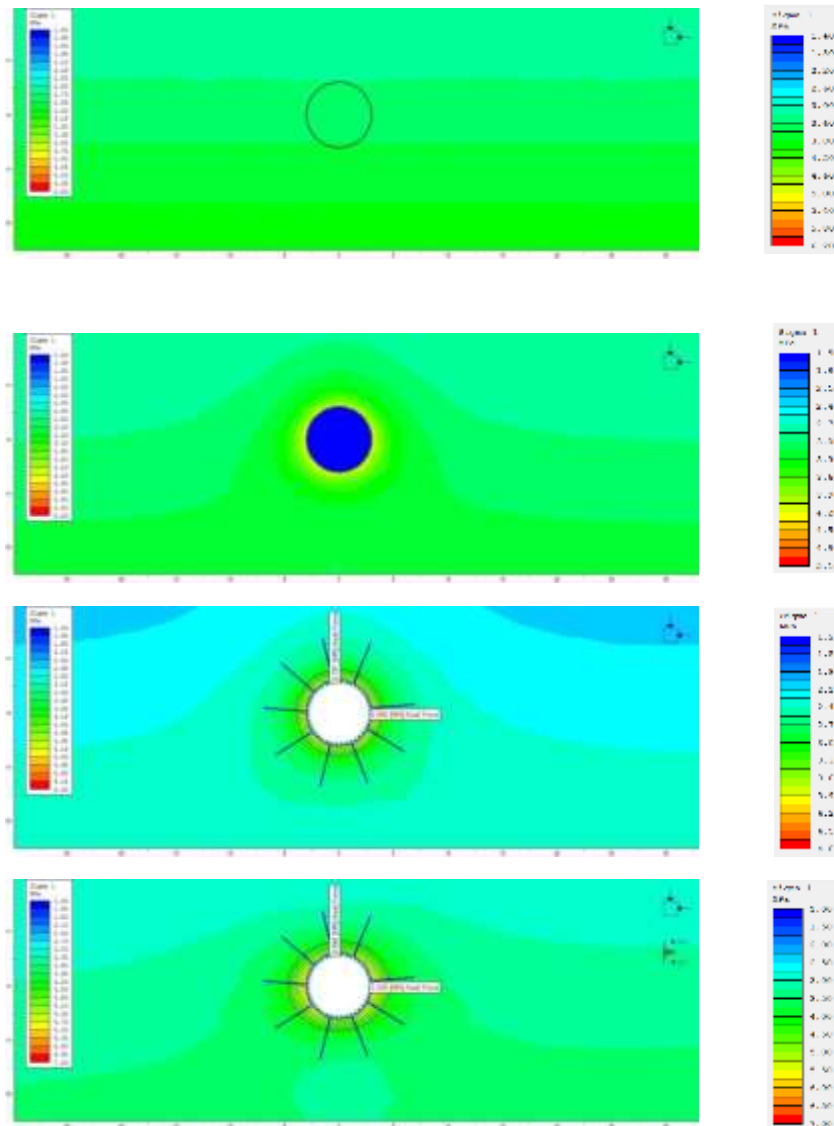
Figure 2 Different stages of simulation in analysis, Stage 1: Consolidation under self weight Stage 2: Stress relaxation using elastic core replacement Stage 3: Static condition Stage 4: Static Loading + Seismic Loading

During tunnel construction, there is always some delay between excavation of the tunnel and installation of the support. Some amount of stress is released before the support is installed such that this portion of the load does not have to borne by the installed support. Therefore, determining the actual magnitude of the load borne by the support system necessitates calculating the amount of stress released during relaxation, or deformation, before the support is installed.

In order to investigate the rock mass-support interaction, a 10-cm thick standard beam liner is placed along the tunnel periphery at this stage; this beam liner simulates a 10-cm thick shotcrete and 4m long rockbolts @2.0×2.0m is applied to support the excavated tunnel. The property of shotcrete which is modeled is shown in Table 3.

Table 3 Support Details

Parameters	Value or description
E Modulus (MPa)	25,000
Poisson's ratio	0.2
Thickness (m)	0.10
Material type	Elastic
Liner Type	Beam and formulated as Timoshenko beam

The effect of earthquake loading on the tunnel can be analysed by taking the difference between the axial force during seismic loading (Stage 4) and the axial force at the same location during static loading (Stage 3). This difference in axial force on the lining, referred to as Seismic Axial Force, can be attributed to the effect of seismic loading during earthquakes and can be used as a parameter to represent the effect of earthquakes.

Discussions

The results of analysis were interpreted in terms of major principal stresses, increase in axial force in the lining after application of seismic load. Fig.3 shows the distribution of major principal stress sigma1 around a 6m tunnel excavated in rock masses with Q ranging from 1 to 30 for elastic-perfectly-plastic models. For the static condition, the high stress zone lies around the invert of the tunnel (~270°), on application of seismic loading, with seismic coefficients K_h = 0.3; K_v = - 0.2, the region of higher stress shifts toward the knee (225°) of the tunnel and another high stress zone develops on the opposite side at the shoulder of the tunnel (45°) resulting two 'ear-like' ellipsoid high stress zones around the tunnel.
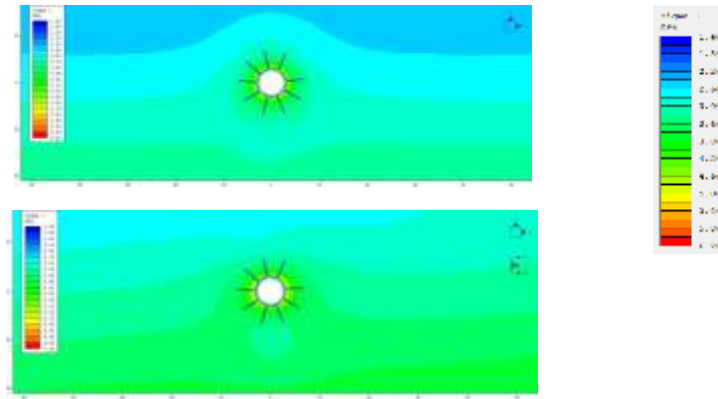
Figure 3 Contour plot of major principal stress sigma 1 around 6m dia. Tunnel with Q=1 for static and seismic condition

The axial force with distanced along the liner for the rock classes for is shown in Fig.4. The axial force on the lining increases with seismic loading. With increasing Q value, the axial force on the lining decreases. The variation of the axial force around the tunnel has some perio-dicity. The seismic axial force along the tunnel circumference for good rock mass with Q = 30 and for poorer rock mass with Q = 1 are shown in Fig. 40. For the good rock mass, the seismic axial force plots are within the same range (>370 kN) indicating that the good rock mass, the increase in axial force as function of tunnel dimension is relatively insignificant.

Furthermore, it may be noted that the increase in the mean axial force due to seismic loading is also significantly larger for Q = 1.
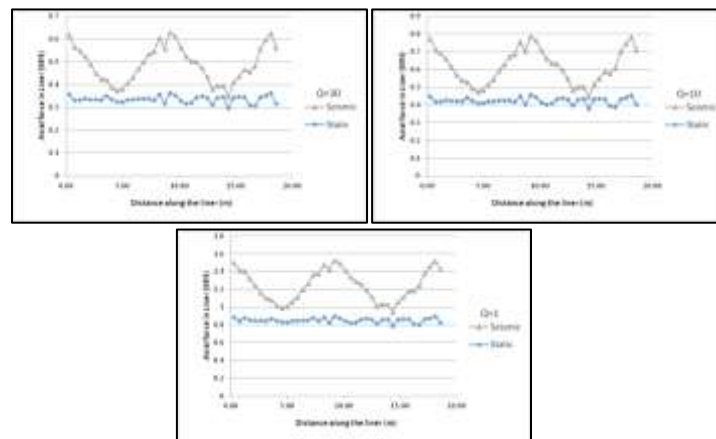
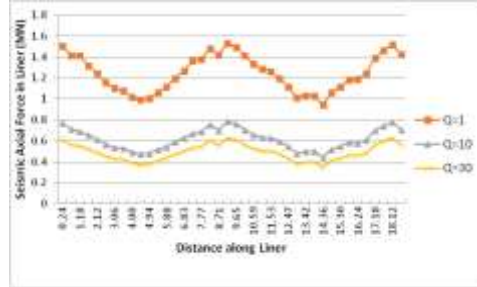Figure 4 Axial force on the lining for both static and seismic loading for with diameter 6 m.

Figure 5 Axial force on the lining for seismic loading for all rock classes

The variation of axial force around the tunnel periphery for tunnel diameter ranging from 6 - 12 m at a depth of 100 m in a rock mass with Q=1 is shown in Fig. 6. It can be inferred that the magnitude of the axial force for both static and seismic loading increases with tunnel dimension for tunnels in poorer quality rock masses with Q=1. The axial force on the lining for tunnels in good quality rock mass with Q=30 also bears the same trend around the tunnel periphery, but the increase in axial force with increasing tunnel dimension is insignificant compared to tunnels in poorer rock mass with Q=1.
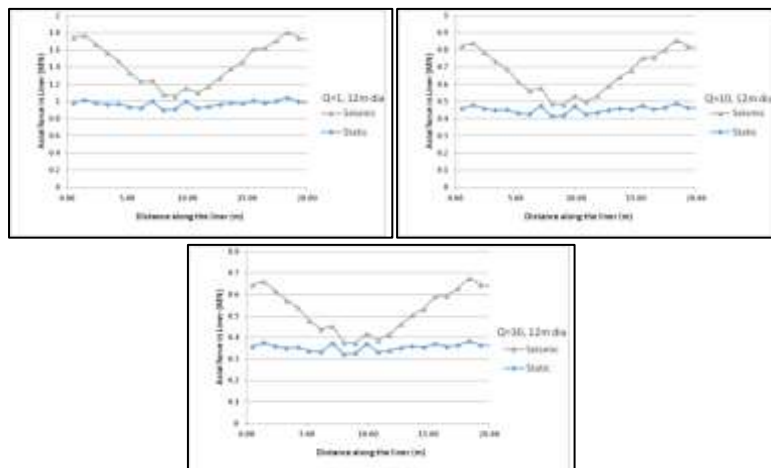
Figure 6 The variation of axial force around the tunnel periphery for tunnel with diameter 12 m and Q ranging 1 - 30.

The effect of discontinuities was investigated using identical loads and material configurations for 12m dia tunnel with Q value 10. The joints were simulated as one at the time in three different inclinations. The inclination was described by an angle from the x axis as in the typical the Cartesian coordinates and in the counter clockwise direction. Based on this, the joints are sometimes refereed at to as 0, 45, and 90 to describe the horizontal, diagonal and vertical joints sequentially. All The joints cross and intersect with the tunnel lining. The joints were given a friction angle =10°, normal and shear stiffness 10000MPa/m and 1000MPa/m successively.

Result and Discussion

Percentage increase in the axial force in the lining for different diameters for rocks without joint is shown below in Table 4

Table 4 Summary of the numerical results for different dia. of tunnel

Q value	Dia. Of Tunnel (m)	Maximum Axial Force in lining for Static Case (MN)	Maximum Axial Force in lining for Seismic Case (MN)	Percent Increase(%)
1	6	0.78	0.94	30.5
10	6	0.37	0.44	15.9
30	6	0.29	0.34	17.2
1	12	0.88	1.03	17.04
10	12	0.40	0.46	15
30	12	0.31	0.36	16.12

The maximum axial force in the shotcrete lining for different values of Q for a single joint with different orientation is given in the Table 5.

Table 5 Summary of the numerical results for different joint inclination

Q value	Dia. Of Tunnel (m)	Maximum Axial Force in lining for Static Case (MN)	Maximum Axial Force in lining for Seismic Case (MN) for Horizontal joint	Maximum Axial Force in lining for Seismic Case (MN) for Vertical joint	Maximum Axial Force in lining for Seismic Case (MN) for diagonal joint
1	6	0.88	1.44	1.54	1.53
10	6	0.44	0.72	0.78	0.79
30	6	0.35	0.58	0.62	0.61
1	12	1.15	1.9	1.8	1.8
10	12	0.49	0.84	0.87	0.85
30	12	0.37	0.66	0.67	0.66

Figures 7 to14 depict a summary of the numerical results for the maximum axial force in lining for the different cases of loading and the different joint orientations. Those figures intend to compare the strong rock and weak rock simulations. For strong rock, the maximum axial

force increases in seismic scenario in comparison to static case. This behaviour is observed regardless of the joint orientation. It was expected that the maximum axial force increases when the medium that enclose the tunnel is weakened by introducing a crossing joint in the tunnel. For the horizontal joint, the locations of the maximum axial force changed after applying seismic loads. The locations of the maximum axial force did not occur at the point of intersection between the horizontal joint and the tunnel lining. The vertical joint simulations produced different locations for the maximum axial force. Similar case is observed for the diagonal joint orientation. As it can be observed from the results of weak rockmass(Q=1), joint weakening effects do not work in a similar way as in the strong rock situation.
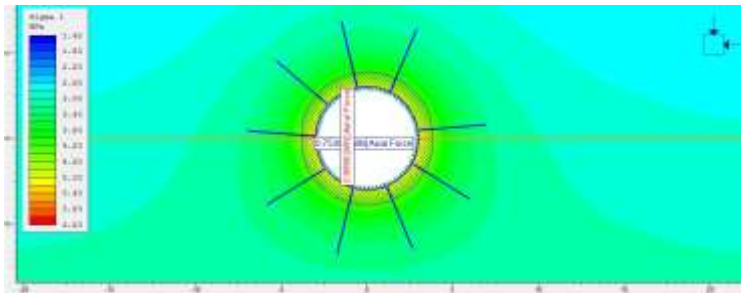
Figure 7   Maximum axial force in lining for weak rock (Q=1) for single horizontal joint simulation for a 6 m diameter circular tunnel under the static loading
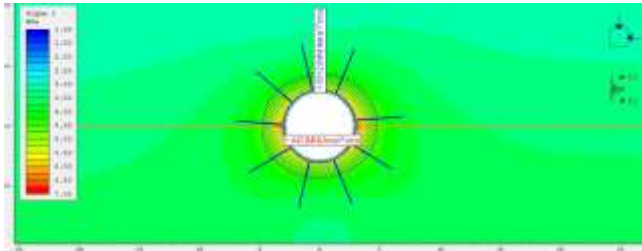

Figure 8 Maximum axial force in lining for weak rock (Q=1) for single horizontal joint simulation for a 6 m diameter circular tunnel after superimposing the seismic load combination
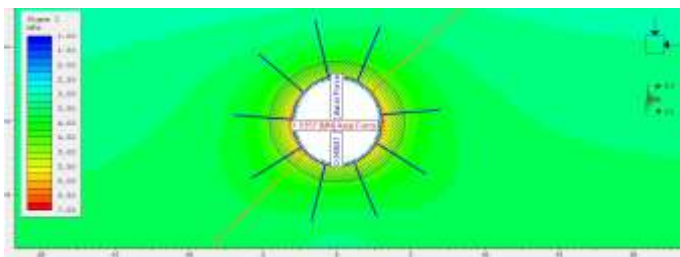

Figure 9 Maximum axial force in lining for weak rock (Q=1) for single diagonal joint simulation for a 6 m diameter circular tunnel after superimposing the seismic load combination
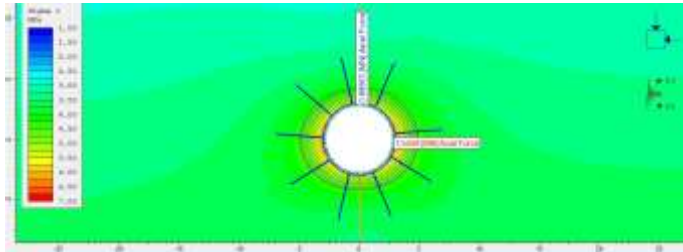
Figure 10 Maximum axial force in lining for weak rock (Q=1) for single vertical joint simulation for a 6 m diameter circular tunnel after superimposing the seismic load combination
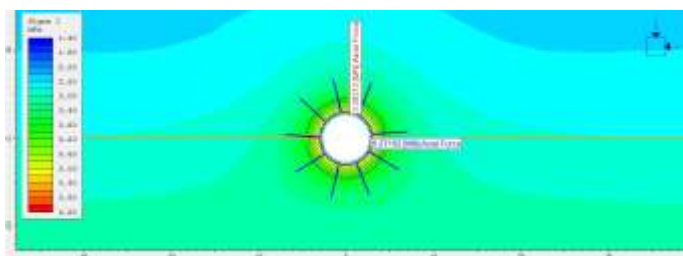

Figure 11 Maximum axial force in lining for strong rock (Q=30) for single horizontal joint simulation for a 6 m diameter circular tunnel under the static loading
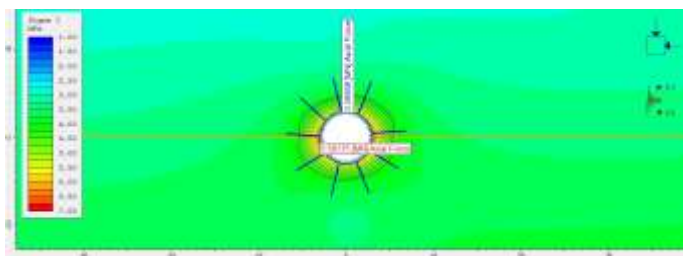

Figure 12 Maximum axial force in lining for strong rock (Q=30) for single horizontal joint simulation for a 6 m diameter circular tunnel after superimposing the seismic load combination
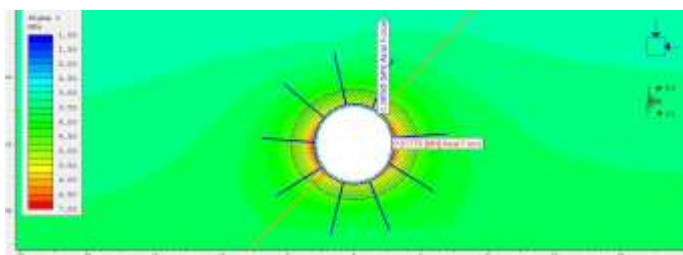

Figure 13 Maximum axial force in lining for strong rock (Q=30) for single diagonal joint simulation for a 6 m diameter circular tunnel after superimposing the seismic load combination
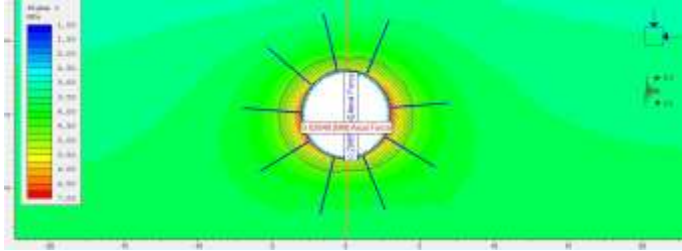
Figure 14 Maximum axial force in lining for strong rock (Q=30) for single vertical joint simulation for a 6 m diameter circular tunnel after superimposing the seismic load combination

References

1. "Insights into the Response of Rock Tunnels to Seismicity" Mostafa Abokhalil, Master Thesis in Geosciences

2. Barton, N., R., Lien, Lunde, J. and 1974. Engineering classification of rockmasses for the design of tunnel support. Rock Mechanics 6(4): 189-236.

3. Bhasin, Kaynia, Paul, Singh and Pal, 2006. Seismic behavior of rock support in tunnels. 13th Symposium on Earthquake Engineering Indian Institute of Technology, Roorkee, 118.

4. Bhasin, R. and Høeg, K. (1998). "Parametric study for a large cavern in jointed rock using a distinct element model (UDEC—BB)." International Journal of Rock Mechanics and Mining Sciences, Vol. 35, No. 1, pp.17-29.

5. Dowding, C. (1979). Earthquake stability of rock tunnels. Tunnels and Tunnelling, pages 15–20.

6. Goel, R. K. "Status of tunnelling and underground construction activities and technologies in India." *Tunnelling and Underground Space Technology* 16.2 (2001): 63-75.

7. Hajiazizi, Mohammad, and Razie Sadat Khatami. "Seismic analysis of the rock mass classification in the Q-system." *International Journal of Rock Mechanics and Mining Sciences* 62 (2013): 123-130.

8. Hashash, Y. M. A., Hook, J. J., Schmidt, B., and Yao, J. I.-C. (2001). Seismic design and analysis of underground structures. Tunnelling and Underground Space Technology, 16(4):247 –293.

9. Hoek, E. and Brown, E. (1997). Practical estimates of rock mass strength. International Journal of Rock Mechanics and Mining Sciences, 34(8):1165–1186.

10. Rajinder Bhasin , Kaare Hoeg and Mostafa Abokhalil, "Effect of seismicity on rock support in tunnels", World Tunnel Congress -2008.